The impact of negative feedback in metabolic noise propagation

Alessandro Borri[1,*], Pasquale Palumbo[1], Abhyudai Singh[2]

[1]Istituto di Analisi dei Sistemi ed Informatica "A. Ruberti", Italian National Research Council (IASI-CNR), Via dei Taurini 19, 00185 Rome, Italy.
E-mail: {alessandro.borri,pasquale.palumbo}.iasi.cnr.it.
[2]Department of Electrical and Computer Engineering, Biomedical Engineering, Mathematical Sciences, Center for Bioinformatics and Computational Biology, University of Delaware, Newark, DE 19716, USA.
E-mail: absingh@udel.edu.
[*]Corresponding author.

Abstract: Synthetic Biology combines different branches of biology and engineering (spanning from biotechnologies to mathematical modeling abstractions), aiming at properly designing synthetic biological circuits, able to replicate emergent properties potentially useful for biotechnology industry, human health and environment. In this note, we investigate the role of negative feedback in noise propagation for a basic (though rather general) enzymatic reaction scheme. Two distinct feedback control schemes on enzyme expression are here considered: one from the final product of the pathway activity, the other from the enzyme accumulation (negative autoregulation). Both the feedback schemes are designed to provide the same steady-state average values of the involved players, in order to evaluate the feedback performances according to the same working mode. Computations are carried out numerically (by means of the Stochastic Simulation Algorithm) and analytically (via Stochastic Hybrid System modeling), the latter allowing to infer information on which model parameter setting leads to a more efficient noise attenuation, according to the chosen feedback scheme. In addition to highlighting the clear role of the feedback in providing a substantial noise reduction, our investigation concludes that the effect of the feedback is enhanced by increasing the promoter sensitivity for both the feedback schemes. A further interesting biological insight is that an increase in the promoter sensitivity provides more benefits to the feedback from the product with respect to the feedback from the enzyme, in terms of enlarging the parameter design space.

1. Introduction

Synthetic biology is a challenging branch of biological research, which aims at exploiting molecular biological techniques, mathematical modeling and forward engineering to suggest the correct wiring (and the proper tuning) to design a synthetic biological circuit, able to replicate emergent properties potentially useful for biotechnology industry, human health and environment [1], [2]. Important results have been recently achieved to isolate and characterize parts of engineered biological circuits, in order to understand how the different modules can be wired in more complex circuits [3]. Modeling takes a leading role in understanding and properly designing such systems, and enables the capability to correctly predict the overall system behavior (see [4] and references

therein).

In this framework, recent attention has been focused on understanding how circuit design may affect metabolic performances, and a pivotal role seems to be played by feedback mechanisms regulating the enzymatic activity. The role of the feedback in systems and synthetic biology has been widely investigated, especially in transcriptional and metabolic regulation where gene products are required to control their homeostatic levels robustly with respect to parameter or environmental fluctuations [5, 6, 7, 8, 9, 10, 11]. Particular attention, in this context, has been devoted to the analysis and the design of stochastic models, able to replicate random oscillations (also generally referred to as *noise*), highlighted by experimental evidence and which cannot be realized by deterministic models [12, 13, 14, 15].

This note investigates the role of the feedback in the enzymatic production rate for a basic (though rather general) metabolic pathway, involving the classical substrate/enzyme binding/unbinding forming a complex that eventually provides a final product (with the release of the enzyme). The feedback on the enzyme is exerted via a transcriptional repression from the product or from the enzyme itself. Both substrate and enzyme productions occur by means of noisy bursts, and the goal is to quantify the level of noise reduction (if any) with respect to the fluctuations (around the steady-state average value) of the final product of the metabolic pathway. A similar study has been proposed in [10] without accounting for noisy burst productions and according to only one feedback scheme. Experimental literature has recently investigated the effects that a negative feedback exerts on noise propagation, especially in gene transcription networks: on the one hand, it is well established that negative autoregulation in gene expression provides attenuation of the stochastic fluctuations of protein numbers [16, 17]; on the other hand, a more intricate relation between feedback and noise propagation is expected, in general, when the negative feedback scheme is compared to the non-regulated control case, because different wirings may vary the steady-state solutions and an amplification of the relative noise (in terms of squared steady-state coefficient of variation of the product normalized to the one generated by a constitutive promoter with the same strength) may occur in spite of a reduction of the fluctuations standard deviation (see, e.g., theoretical and experimental results in [10] and [13], respectively). To avoid this ambiguity, here the comparison among the feedback schemes (and the constitutive case without feedback) is performed by keeping fixed the steady-states average values of the players (which, on the other hand, may well vary according to the strength and sensitivity of the feedback). To this end, feedback parameters are tuned in order to provide the same stationary solutions for the three schemes under investigation (two feedback schemes in addition to the constitutive one): from a synthetic biology perspective we aim at investigating the noise propagation related to different ways to provide the same metabolic working mode (related to the same steady-state solutions).

A proper way to quantify the metabolic noise involving the product fluctuations around the steady-state average value is to exploit the stochastic approach based on the Chemical Master Equations (CME), providing a description of complex cellular processes much more accurate than the deterministic one [18]. CMEs are capable of coping with fluctuations and chemical fluxes, to fit experimental data in the currently widespread single cell experiments, and of capturing and explaining the deviation from Gaussianity observed in various gene expression experiments (such as stress or metabolic response, growth of the nuclear protein amount observed in senescent cells, and so on). However, a major problem in dealing with CME is the *curse of dimensionality* which, in many cases, prevents from explicitly computing the solutions and thus requires implementing efficient algorithms [19] or Monte Carlo methods (e.g. the Gillespie Stochastic Simulation Algorithm (SSA) [20]) to estimate the stationary distribution. Moreover, in the case of enzymatic

reactions, the double time-scale of the reactions involved (binding/unbinding reactions occur on a shorter time-scale than product formation and enzyme production) makes exact SSA computationally demanding, since it gets stuck on thousands of binding/unbinding reactions for each birth of a product molecule [10]. As a matter of fact, we adopt here the *slow-scale Stochastic Simulation Algorithm* (ss-SSA) [21, 22], which is an approximate accelerated implementation of SSA, properly exploiting the time scale separation to obtain reliable results within reasonable computation times. These simulations will be considered as the baseline to validate any other level of abstraction proposed in the paper, and confirm the unequivocal role of the feedback in providing a quantitative noise reduction.

In addition to the numerical results provided by the ss-SSA, we aim at determining under which setting of the model parameters one of the two feedback schemes provides better improvements in noise reduction. To this end, analytical solutions should be pursued and proper approximation schemes are invoked. Linear Noise Approximation (LNA) is one of the most adopted frameworks [18] and is substantially derived from the CME after linearization of the nonlinear propensities. Such an approach has been exploited in [11] to compute the stationary value of the product noise variance, but the final formulas revealed to be still cumbersome to use and little informative. Differently from [11], here a Stochastic Hybrid System (SHS) [23] is adopted to derive analytical solutions, entailing both continuous and discrete events: the latter are provided by the noisy enzyme and substrate production, whilst the players' copy number is supposed to continuously vary between individual burst events, according to a deterministic Ordinary Differential Equation (ODE) framework. This is a typical approach adopted whenever the contribution of the bursty production is dominant with respect to the other reactions (e.g. because of a high average burst size) [24]. A tool providing the noise variations around the steady state solutions is the moment equation approach for SHS [23], but it cannot be straightforwardly applied in presence of saturation functions (a typical assumption in Systems Biology [8]) and, in any case, it requires linear propensities for the involved reactions in order to obtain solvable closed-form equations (this drawback can be overcome by means of moment closure techniques [25]). To cope with such problems, we linearize the nonlinear propensities with respect to the average steady-state copy numbers of the players, allowing to write the moment equations in a closed form and to obtain solutions which, unfortunately, are still hard to handle and cannot be written in an easy analytical fashion. To this end, a further approximation is considered, suitably exploiting the double time scale of the system, typical of enzymatic reactions, which is finally able to provide simpler analytical expressions allowing to explicitly correlate the metabolic noise of the product to the model parameters. These solutions can be exploited to understand which model parameter setting leads to a more efficient noise attenuation, according to the chosen feedback scheme.

2. Chemical reaction schemes

The chemical reaction scheme under investigation is the one reported in Fig. 1, and will be referred to, in the sequel, as *scheme 0*. It consists of a *substrate* S binding to an *enzyme* E in order to form a *complex* C (reaction 1), which in turn can reverse the binding (reaction 2) or can be transformed into a *product* P with the release of the enzyme E (reaction 3). The reaction scheme accounts for enzyme production (reaction 4) and degradation (reaction 5), product elimination (for instance due to its final utilization, reaction 6) and substrate production (reaction 7). With respect to the enzyme production, in addition to scheme 0 where there is no feedback regulation, two different feedback schemes will be investigated: *scheme 1*, where the enzyme production

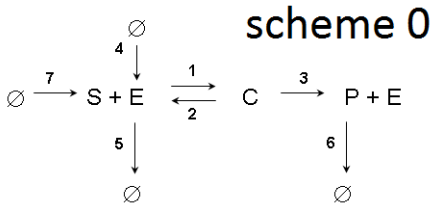

Fig. 1. *Scheme 0: general reaction framework without feedback on the enzyme production*

involves a negative feedback regulation from the product P, and *scheme 2*, where the enzyme production is negatively regulated in feedback by the enzyme E itself (Fig. 2). A similar reaction

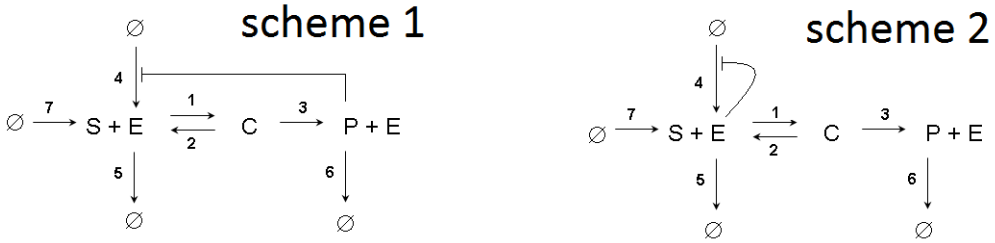

Fig. 2. *Feedback schemes: enzyme production is negatively regulated by a feedback from the product (scheme 1) or from the enzyme itself (scheme 2)*

scheme has been investigated also in [10], where only the feedback from the product on the enzyme production had been considered (instead of the present two feedback schemes); moreover, here also the substrate production has been taken into account (instead of keeping it constant in copy number, as in [10]). Finally, substrate and enzyme production rates are here modeled by means of noisy bursts of B_e and B_s copy numbers, respectively, with the random variables B_e and B_s indicating the size (in terms of number of copies) of the bursts, occurring with probabilities $\mathbb{P}(B_e = i)$ and $\mathbb{P}(B_s = j)$, with $i, j \in \{0, 1, \ldots\}$.

As in [26, 27] we assume geometric probability distributions:

$$\mathbb{P}(B_x = i) = (1 - \lambda_x)^i \lambda_x, \qquad \lambda_x \in (0, 1], \qquad i = 0, 1, \ldots, \qquad x = e, s \tag{1}$$

providing an average burst size $\langle B_x \rangle = (1 - \lambda_x)/\lambda_x$.

According to the standard stochastic approach to chemical reaction modeling [18], the state of the system is identified by the copy number of each involved species $n_s(t)$, $n_e(t)$, $n_c(t)$, $n_p(t)$, and the temporal evolution of a reaction network is described by a Continuous-Time Markov Process, where a state-dependent *propensity* w_j is associated to each reaction j. Table 1 summarizes the players population resets associated to each reaction, and reports the associated propensities. All propensities (except the ones related to the feedback schemes) are written according to the mass action law, so the only nonlinearity is related to the binding reaction (proportional to the product of the involved species).

Regarding the enzyme production for both the feedback schemes, sigmoidal Hill functions are considered, whose value decreases with the product (function $f_1(n_p)$ in scheme 1) or with the

Table 1 Table of reactions: the first column describes the reaction-based event, the second refers to the corresponding reset on the players population, and the third reports the associated propensity function

Event	Population reset	Propensity function
substrate/enzyme binding	$n_s(t) \mapsto n_s(t) - 1$ $n_e(t) \mapsto n_e(t) - 1$ $n_c(t) \mapsto n_c(t) + 1$	$k_1 n_s(t) n_e(t)$
substrate/enzyme unbinding	$n_s(t) \mapsto n_s(t) + 1$ $n_e(t) \mapsto n_e(t) + 1$ $n_c(t) \mapsto n_c(t) - 1$	$k_2 n_c(t)$
product production/enzyme release	$n_e(t) \mapsto n_e(t) + 1$ $n_c(t) \mapsto n_c(t) - 1$ $n_p(t) \mapsto n_p(t) + 1$	$k_3 n_c(t)$
burst enzyme production (scheme 0)	$n_e(t) \mapsto n_e(t) + i,\ i = 0, 1, \ldots$	$k_4 \mathbb{P}(B_e = i)$
burst enzyme production (scheme 1)	$n_e(t) \mapsto n_e(t) + i,\ i = 0, 1, \ldots$	$f_1\big(n_p(t)\big) \mathbb{P}(B_e = i)$
burst enzyme production (scheme 2)	$n_e(t) \mapsto n_e(t) + i,\ i = 0, 1, \ldots$	$f_2\big(n_e(t)\big) \mathbb{P}(B_e = i)$
enzyme degradation	$n_e(t) \mapsto n_e(t) - 1$	$k_5 n_e(t)$
product export	$n_p(t) \mapsto n_p(t) - 1$	$k_6 n_p(t)$
burst substrate production	$n_s(t) \mapsto n_s(t) + i,\ i = 0, 1, \ldots$	$k_7 \mathbb{P}(B_s = i)$

enzyme (function $f_2(n_e)$ in scheme 2):

$$f_1(n_p) = \frac{\beta_1}{1 + (n_p/\theta_1)^{h_1}}, \qquad f_2(n_e) = \frac{\beta_2}{1 + (n_e/\theta_2)^{h_2}}. \tag{2}$$

Parameters β_1 and β_2 provide the maximal propensities (the *promoter strengths*), obtainable for negligible values of their entries n_p and n_e. The propensities reach half of their maximal values in correspondence of the *repression thresholds*, θ_1 and θ_2, respectively. Parameters h_1, h_2 are the *promoter sensitivities*, affecting the steepness of the sigmoidal functions.

Referring to the product P, we define the corresponding metabolic noise by means of the square of the coefficient of variation CV_P^2 computed by the ratio:

$$CV_P^2 = \sigma_P^2 / (n_p^\star)^2 \tag{3}$$

where σ_P^2 and $n_p^\star$ are the steady-state values for variance and mean of the marginal distribution of the product P copy number [10].

In the following, unless differently specified, the expected value of a random variable x will be denoted by $\langle x \rangle$, while the steady-state average value of a stochastic process $x(t)$ will be denoted by $x^\star = \lim_{t \mapsto +\infty} \langle x(t) \rangle$.

3. Average steady-state solutions

The computation of the average steady-state solution plays a central role in our investigation, since we aim at quantifying the noise propagation for different wiring schemes, all sharing the same average steady-state solution (i.e. the same stationary working modes). The first-order moment

equations derive from the Chemical Master Equations according to [23]. Unfortunately, the nonlinearities involved in the complex formation, as well as in the enzyme production for the feedback schemes, do not allow to achieve closed-form solutions. Indeed, the nonlinear terms provided by the negative feedback schemes even prevent to use the moment closure techniques [25]. Therefore, computations will be carried out according to the linearization of the nonlinear propensities around the stationary average values $n_s^\star, n_e^\star, n_p^\star$:

$$\begin{aligned} k_1 n_s(t) n_e(t) &\simeq k_1\Big(n_s^\star n_e^\star + n_e^\star\big(n_s(t)-n_s^\star\big) + n_s^\star\big(n_e(t)-n_e^\star\big)\Big), \\ f_1\big(n_p(t)\big)\mathbb{P}(B_e=i) &\simeq \Big(f_1(n_p^\star) + f_1'(n_p^\star)\big(n_p(t)-n_p^\star\big)\Big)\mathbb{P}(B_e=i), \\ f_2\big(n_e(t)\big)\mathbb{P}(B_e=i) &\simeq \Big(f_2(n_e^\star) + f_2'(n_e^\star)\big(n_e(t)-n_e^\star\big)\Big)\mathbb{P}(B_e=i). \end{aligned} \tag{4}$$

According to [23], the first order moment equations can be written in a unified fashion for the three schemes, with the steady-state solutions obeying the following system:

$$\begin{aligned} &-k_1 n_s^\star n_e^\star + k_2 n_c^\star + k_7\langle B_s\rangle = 0 \\ &-k_1 n_s^\star n_e^\star + (k_2+k_3) n_c^\star - k_5 n_e^\star + \chi(n_p^\star, n_e^\star)\langle B_e\rangle = 0 \\ &k_1 n_s^\star n_e^\star - (k_2+k_3) n_c^\star = 0 \\ &k_3 n_c^\star - k_6 n_p^\star = 0 \end{aligned} \tag{5}$$

with

$$\chi(n_p^\star, n_e^\star) = \begin{cases} k_4, & \text{scheme 0}, \\ f_1(n_p^\star), & \text{scheme 1}, \\ f_2(n_e^\star), & \text{scheme 2}. \end{cases} \tag{6}$$

From standard computations, the steady state solutions of (5) satisfy:

$$n_p^\star = \frac{k_7\langle B_s\rangle}{k_6}, \qquad n_c^\star = \frac{k_6}{k_3} n_p^\star, \qquad n_e^\star = \frac{\chi(n_p^\star, n_e^\star)\langle B_e\rangle}{k_5}, \qquad n_s^\star = \frac{(k_2+k_3) n_c^\star}{k_1 n_e^\star}, \tag{7}$$

for which existence and uniqueness of the solutions are clearly ensured whatever the chosen scheme and the model parameters.

It is readily seen that the feedback on the enzyme production (schemes 1 and 2) does not vary the product and complex steady-state solutions with respect to the constitutive case (scheme 0). In fact, product and complex steady-state solutions are not affected by the enzyme production at all. Instead, the enzyme production rate influences the enzyme and substrate steady-state solutions. In case of schemes 0 and 1, $n_e^\star$ is achieved in closed form

$$n_e^\star(\text{scheme 0}) = \frac{k_4\langle B_e\rangle}{k_5}, \qquad n_e^\star(\text{scheme 1}) = \frac{f_1(n_p^\star)\langle B_e\rangle}{k_5}, \tag{8}$$

whilst, in case of scheme 2, $n_e^\star$ is numerically provided by the solution of the equation

$$n_e^\star = \frac{f_2(n_e^\star)\langle B_e\rangle}{k_5}. \tag{9}$$

Therefore, if we want to achieve the same steady-state solution for the three different schemes, we need to tune the feedback parameters in order to get:

$$f_1(n_p^\star) = f_2(n_e^\star) = k_4, \qquad \text{with} \qquad n_p^\star = \frac{k_7\langle B_s\rangle}{k_6} \quad \text{and} \quad n_e^\star = \frac{k_4\langle B_e\rangle}{k_5}. \tag{10}$$

Table 2 Model parameters. Measurement units: k_1, [s^{-1}molecule^{-1}]; k_x, $x = 2, 3, \ldots, 7$, [s^{-1}].

Parameter	k_1	k_2	k_3	k_4	k_5	k_6	k_7	λ_e	λ_s
Value	1	28300	3.2	0.16	0.02	0.02	2.4	0.25	0.15

Note that, for fixed values of the promoter sensitivities h_1, h_2, and of the steady-states $n_p^\star$, $n_e^\star$, promoter strengths β_1, β_2 and repression thresholds θ_1, θ_2 are constrained by (10) to given curves. Some of these curves are reported in Fig. 3, according to parameters given by Table 2.

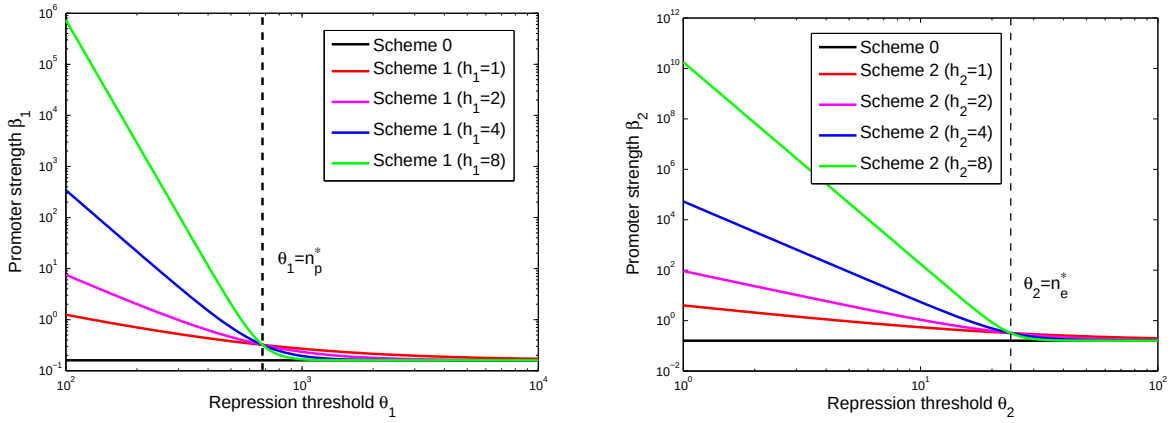

Fig. 3. *(β, θ)-curves ensuring fixed values of $n_e^\star = k_4 \langle B_e \rangle / k_5$ for different values of the promoter sensitivity h. Left panel refers to function $f_1(n_p)$, right panel refers to function $f_2(n_e)$.*

It clearly appears that by making the value of the threshold θ_1 much larger than $n_p^\star$ for scheme 1 (and θ_2 much larger than $n_e^\star$ for scheme 2), the inhibitory action of the feedback becomes weaker and weaker and the promoter strengths β_1, β_2, rapidly approach the value k_4: for $\theta_1 \gg n_p^\star$ and $\theta_2 \gg n_e^\star$, both feedback schemes behave similarly to the constitutive case of scheme 0. Instead, by making θ_1 much smaller than $n_p^\star$ for scheme 1 (and θ_2 much smaller than $n_e^\star$ for scheme 2), the inhibitory action of the feedback becomes stronger and stronger, and the promoter strengths β_1, β_2 are required to dramatically increase their value to guarantee the same enzyme production rate (and the same enzyme stationary average value). By increasing the promoter sensitivities, such biphasic behavior becomes more and more evident. Finally, note that, similarly to [10], here we account for promoter sensitivities exceeding the typical bound values of 4 or 5. Motivation for that stems from recent synthetic biology experimental work (see, e.g., [28]), where protein sequestration mechanisms allow to produce a sharp ultrasensitive response with an apparent Hill coefficient far beyond standard values.

4. Second-order moments and computation of the metabolic noise

4.1. Numerical solutions

As discussed in Section 1, the explicit computation of the exact steady-state distribution and average values of the three reaction schemes is unfeasible, due to the large number of molecules

involved. Moreover, the standard Gillespie SSA [20] is inefficient in view of obtaining an equilibrium statistical distribution due to the inherent double time scale of the reaction network. As a consequence, the slow-scale Stochastic Simulation Algorithm (ss-SSA) [21] has been implemented in Matlab and the following average steady-state solutions have been obtained (after 10^6 Monte Carlo runs of the algorithm), according to the parameter setting defined in Table 2:

$$n_s^\star = 5012, \qquad n_e^\star = 24, \qquad n_c^\star = 4.25, \qquad n_p^\star = 680. \tag{11}$$

Feedback parameters have been set by varying the promoter sensitivities $h_1, h_2 \in \{1, 2, 4, 8\}$ and the repression thresholds $\theta_1 \in [10^2,\ 10^4]$ and $\theta_2 \in [10^0,\ 10^2]$, while the promoter strengths β_1, β_2 are uniquely defined by (10) (see also Fig. 3). Simulations results are reported in Fig. 4 where each circle comes out from a set of ss-SSA runs associated to a specific pair of (θ_1, h_1) for scheme 1 and of (θ_2, h_2) for scheme 2.

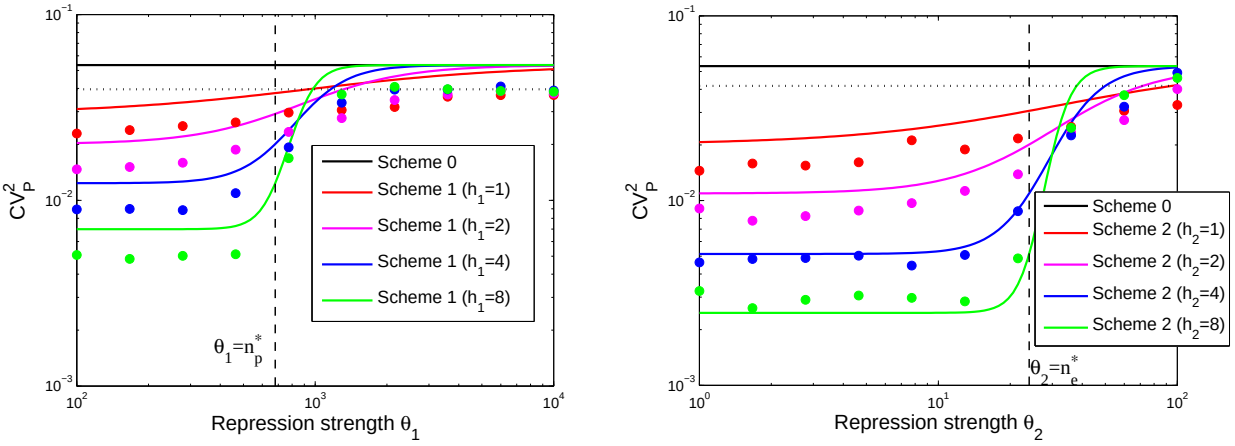

Fig. 4. *Metabolic noise for different values of pairs (θ, h), scheme 1 (left) and scheme 2 (right). The solid lines are referred to the SHS formulation. The dotted line (scheme 0) and the circles (feedback schemes 1 and 2) are obtained by means of the slow-scale Stochastic Simulation Algorithm.*

According to reported simulations, both feedback schemes seem to share the same significant properties, summarized as follows:

– both feedback schemes 1 and 2 reduce noise propagation with respect to the constitutive case of scheme 0, whatever the chosen feedback parameters constrained by (10);

– by noticeably increasing the repression thresholds with respect to the corresponding average steady-states ($\theta_1 \gg n_p^\star$, $\theta_2 \gg n_e^\star$), the noise reduction attenuates and eventually vanishes: the ss-SSA suggests that the two feedback schemes become indistinguishable with respect to the constitutive case for much larger values of the repression threshold;

– by noticeably decreasing the repression thresholds with respect to the corresponding average steady-states ($\theta_1 \ll n_p^\star$, $\theta_2 \ll n_e^\star$), the noise reduction strongly benefits of the feedback scheme: the ss-SSA suggests that the CV_P^2 eventually approaches an asymptotic value for much smaller values of the repression threshold;

– by increasing the promoter sensitivities h_1, h_2, such a behavior is enhanced, making the CV_P^2-vs-θ curves steeper and steeper.

4.2. Analytical solutions

In order to infer information on which model parameter setting leads to a more efficient noise attenuation according to the chosen feedback scheme, we need to relate the metabolic noise to the feedback parameters. To this end, we exploit the linearization adopted for the binding reaction propensity and for the feedback control functions on the enzyme production rate in (4), already employed to provide the first-order steady-state solutions. First attempts in this direction have been carried out in [11] by properly exploiting the Quasi Steady-State Approximation (QSSA) in the Linear Noise Approximation (LNA) framework, according to a particular combination of the feedback parameters. Unfortunately, the final formulas revealed to be still cumbersome to use and little informative.

Instead, here we provide analytical solutions to the metabolic noise by means of a Stochastic Hybrid System (SHS) model of the reaction network. At the SHS level of abstraction, the players' copy numbers are modeled by means of continuous state variables, evolving according to deterministic ODEs involving all reactions with the exception of burst productions. According to the linearized propensities in (4), the ODE system evolving between any two bursts of enzyme/substrate production is

$$\begin{aligned}
\dot{n}_s(t) &= -k_1\big(n_s^\star n_e^\star + n_e^\star\big(n_s(t)-n_s^\star\big) + n_s^\star\big(n_e(t)-n_e^\star\big)\big) + k_2 n_c(t)\\
\dot{n}_e(t) &= -k_1\big(n_s^\star n_e^\star + n_e^\star\big(n_s(t)-n_s^\star\big) + n_s^\star\big(n_e(t)-n_e^\star\big)\big) + (k_2+k_3) n_c(t) - k_5 n_e(t)\\
\dot{n}_c(t) &= k_1\big(n_s^\star n_e^\star + n_e^\star\big(n_s(t)-n_s^\star\big) + n_s^\star\big(n_e(t)-n_e^\star\big)\big) - (k_2+k_3) n_c(t)\\
\dot{n}_p(t) &= k_3 n_c(t) - k_6 n_p(t).
\end{aligned} \tag{12}$$

Algebraic equations providing the first-order steady-state solutions coming from (12) (accounting also for the burst production of substrate and enzyme, [23]) coincide with the ones provided by the CME in (5). On the other hand, equations for second order moments vary. From a numerical viewpoint, the use of the SHS dramatically simplifies the computational burden, and it is computationally inexpensive to draw the continuous lines for CV_P^2 as reported in Fig. 4. It can be appreciated that the SHS approach nicely reproduces the qualitative behavior, keeping a satisfactory quantitative correspondence with the ss-SSA numerical values.

Unfortunately, the use of an SHS model does not reduce the complexity of seeking the analytical solutions, since the stationary second-order moments are related to the solutions of a 10th-order system. To reduce such a complexity, the Quasi-Steady-State Approximation (QSSA) is adopted and applied to the deterministic equations given by (12). The QSSA is a widespread approach employed to reduce the computational complexity in the presence of a typical fast/slow timescale of enzymatic reactions: see e.g. [29, 30] and references therein for an exhaustive review of advantages and limitations of such approach, which substantially exploits the faster dynamics of complex C, supposed to be negligible (i.e. $\dot{n}_c = 0$) with respect to the other players' dynamics. By setting $\dot{n}_c = 0$ and substituting the expression of the complex n_c in terms of the other three players, the ODE system reduces to:

$$\begin{aligned}
\dot{n}_s(t) &= -\tfrac{k_1 k_3}{k_2+k_3}\big(n_s^\star n_e^\star + n_e^\star\big(n_s(t)-n_s^\star\big) + n_s^\star\big(n_e(t)-n_e^\star\big)\big)\\
\dot{n}_e(t) &= -k_5 n_e(t)\\
\dot{n}_p(t) &= \tfrac{k_1 k_3}{k_2+k_3}\big(n_s^\star n_e^\star + n_e^\star\big(n_s(t)-n_s^\star\big) + n_s^\star\big(n_e(t)-n_e^\star\big)\big) - k_6 n_p(t).
\end{aligned} \tag{13}$$

The QSSA does not affect the stationary mean values; instead it modifies the steady-state second-order moments, which are the solutions of a 6th-order linear system. After some computations, we

find the following expressions for the CV_P^2 for the basic scheme 0:

$$CV_P^2 = \frac{1}{2\left(1+\frac{n_p^\star}{n_s^\star}\right)}\left[\frac{\langle B_s^2\rangle}{\langle B_s\rangle\, n_s^\star} + \frac{\langle B_e^2\rangle}{\langle B_e\rangle\, n_e^\star}\cdot\frac{k_5k_6}{(k_5+k_6)\left(k_5+k_6\frac{n_p^\star}{n_s^\star}\right)}\right]. \tag{14}$$

Because of the geometric distribution of B_x, $x = s, e$, the following equality holds:

$$\frac{\langle B_x^2\rangle}{\langle B_x\rangle} = 1 + 2\langle B_x\rangle, \qquad x = s, e \tag{15}$$

so that (14) reduces to:

$$CV_P^2 = \frac{1}{2\left(1+\frac{n_p^\star}{n_s^\star}\right)}\left[\frac{1+2\langle B_s\rangle}{n_s^\star} + \frac{1+2\langle B_e\rangle}{n_e^\star}\cdot\frac{k_5k_6}{(k_5+k_6)\left(k_5+k_6\frac{n_p^\star}{n_s^\star}\right)}\right] \tag{16}$$

from which it is apparent that (16) is constituted by the sum of two contributes in the square brackets:

– the former depends on both the noise sources since, according to (7), one has:

$$\frac{1+2\langle B_s\rangle}{n_s^\star} = \frac{k_1k_3n_e^\star}{k_7(k_2+k_3)}\cdot\frac{1+2\langle B_s\rangle}{\langle B_s\rangle} = \frac{k_1k_3k_4\langle B_e\rangle}{k_5k_7(k_2+k_3)}\cdot\frac{1+2\langle B_s\rangle}{\langle B_s\rangle}; \tag{17}$$

– the latter depends of only the enzyme production noise source, since:

$$\frac{1+2\langle B_e\rangle}{n_e^\star} = \frac{k_5}{k_4}\cdot\frac{1+2\langle B_e\rangle}{\langle B_e\rangle} \qquad \text{and} \qquad \frac{n_p^\star}{n_s^\star} = \frac{k_1k_3k_4}{k_5k_6(k_2+k_3)}\langle B_e\rangle. \tag{18}$$

The shape of (16)-(18) allows to investigate the role of the burst sizes $\langle B_s\rangle$ and $\langle B_e\rangle$ in metabolic noise. Small values of $\langle B_s\rangle$ proportionally reduce $n_s^\star$, thus making the former contribute (17) preponderant with respect to the latter, which does not depend of $\langle B_s\rangle$; moreover by making $\langle B_s\rangle$ smaller and smaller, CV_P^2 becomes larger and larger because of (17). Instead, by increasing $\langle B_s\rangle$, $n_s^\star$ proportionally increases allowing (17) to eventually reach an asymptotic value, which may well be comparable with the latter contribute. Regarding the role of $\langle B_e\rangle$, it works on both the addends in the square brackets. Then, small values of $\langle B_e\rangle$ proportionally reduce $n_e^\star$, thus making the latter contribute preponderant with respect to the former, which, on the contrary, reduces proportionally with $\langle B_e\rangle$; moreover, similarly to the case of $\langle B_s\rangle$, by making $\langle B_e\rangle$ smaller and smaller, CV_P^2 becomes larger and larger because of (18). Instead, by increasing $\langle B_e\rangle$, then $n_p^\star/n_s^\star \mapsto +\infty$, so the latter contribute vanishes, whilst (17) becomes arbitrarily large: the former contribute becomes preponderant but the CV_P^2 definitely reaches an asymptotic value, which depends of $\langle B_s\rangle$:

$$\lim_{\langle B_e\rangle\mapsto+\infty} CV_P^2 = \frac{k_6}{2k_7}\cdot\frac{1+2\langle B_s\rangle}{\langle B_s\rangle} = \frac{1+2\langle B_s\rangle}{2n_p^\star}. \tag{19}$$

A further simplification exploits again the double time scale property in metabolic reactions, characterized by very small values of the ratio $\epsilon = k_3/k_2 \ll 1$ (see, e.g., [22]). According to the steady-state solutions (7), this straightforwardly leads to

$$\frac{n_p^\star}{n_s^\star} \simeq \epsilon_1 = \epsilon\frac{k_1k_4\langle B_e\rangle}{k_5k_6} \qquad\qquad \frac{n_e^\star}{n_s^\star} \simeq \epsilon_2 = \epsilon\frac{k_1k_4^2\langle B_e\rangle^2}{k_5^2k_7\langle B_s\rangle} \tag{20}$$

so that CV_P^2 can be written as:

$$CV_P^2 = \frac{1}{2n_e^\star\big(1+\epsilon_1\big)}\left[\epsilon_2\left(1+2\left\langle B_s\right\rangle\right)+\frac{k_5k_6\left(1+2\left\langle B_e\right\rangle\right)}{(k_5+k_6)(k_5+k_6\epsilon_1)}\right]. \tag{21}$$

In summary, whenever the double time scale property is apparent ($\epsilon \mapsto 0$), the noise coming from the substrate burst production becomes more and more negligible (since it is multiplied by $\epsilon_2 \mapsto 0$), thus assigning to the enzyme burst noisy production a major role in noise propagation. Furthermore, according to (21), when $\epsilon \mapsto 0$, the CV_P^2 simplifies into:

$$CV_P^2 \simeq \frac{k_6\left(1+2\left\langle B_e\right\rangle\right)}{2n_e^\star(k_5+k_6)} = \frac{1+2\left\langle B_e\right\rangle}{2\left\langle B_e\right\rangle}\cdot\frac{k_5k_6}{k_4(k_5+k_6)}. \tag{22}$$

Hence, small values of the burst size of the enzyme production provide an increase in the metabolic noise, because of the corresponding reduction in the steady-state enzyme average value. Instead, for large values of $\langle B_e\rangle$, the approximated formula in (22) is no longer valid, in general, since ϵ_2 is proportional to $\langle B_e\rangle$, and we need to exploit (19).

4.3. Noise reduction due to a feedback from the product (scheme 1)

According to the QSSA applied to the SHS model, the CV_P^2 of scheme 1 can be written (after some computations) as follows:

$$CV_P^2(\text{scheme 1}) = \frac{CV_P^2(\text{scheme 0})}{\Gamma}, \tag{23}$$

with

$$\Gamma = 1+\frac{h_1(n_p^\star)^{h_1}}{\theta_1^{h_1}+(n_p^\star)^{h_1}}\cdot\frac{1}{1+\frac{n_p^\star}{n_s^\star}}\cdot\frac{k_5+k_6\big(1+\frac{n_p^\star}{n_s^\star}\big)}{k_5+k_6\frac{n_p^\star}{n_s^\star}}\cdot\frac{k_5}{k_5+k_6}. \tag{24}$$

As a matter of fact, it clearly comes that $CV_P^2(\text{scheme 1}) < CV_P^2(\text{scheme 0})$ because $\Gamma > 1$ for any choice of the model parameters: the feedback from the product on the enzyme production reduces the noise in the product fluctuations. These results are qualitatively and quantitatively in agreement with those provided by the SHS without QSSA.

Getting in the details of (23)–(24), it comes that:

– by increasing θ_1 with respect to $n_p^\star$ ($\theta_1 \gg n_p^\star$), the effect of the feedback on the noise reduction attenuates, since $\Gamma \mapsto 1$ and, straightforwardly, $CV_P^2(\text{scheme 1}) \mapsto CV_P^2(\text{scheme 0})$; instead, by decreasing θ_1 with respect to $n_p^\star$ ($\theta_1 \ll n_p^\star$), the effect of the feedback on the noise reduction is enhanced and, by accounting for the simplifying assumptions provided by (20), when $\theta_1/n_p^\star \mapsto 0$ and $\epsilon \simeq 0$, one gets:

$$\Gamma \mapsto 1+h_1 \qquad \Longrightarrow \qquad CV_P^2(\text{scheme 1}) \mapsto \frac{CV_P^2(\text{scheme 0})}{1+h_1}. \tag{25}$$

Such a qualitative behavior for varying values of θ_1 is coherent with data shown in Fig.4, left panel, according to the ss-SSA and SHS without QSSA;

– lower and lower values of the substrate average burst size $\langle B_s \rangle$ proportionally decrease $n_p^\star$ (keeping unchanged the ratio $n_p^\star/n_s^\star$) thus making it so that $\Gamma \mapsto 1$; higher and higher values of the enzyme average burst size $\langle B_e \rangle$ proportionally increase the ratio $n_p^\star/n_s^\star$ making it so that $\Gamma \mapsto 1$: too low values of $\langle B_s \rangle$ or too high values of $\langle B_e \rangle$ may vanish the feedback effect in terms of noise reduction;

– the approximation in (20), provided that $k_3/k_2 \ll 1$, further simplifies the equation for Γ:

$$\Gamma = 1 + \frac{h_1 (n_p^\star)^{h_1}}{\theta_1^{h_1} + (n_p^\star)^{h_1}}, \tag{26}$$

hence making the feedback dependent only of the substrate burst noise source.

– the promoter sensitivity h_1 enhances the effect of the feedback, especially for low values of the repression threshold θ_1.

4.4. Noise reduction due to a feedback from the enzyme (Scheme 2)

According to the QSSA applied to the SHS model, the CV_P^2 of scheme 2 can be written (after computations) as follows:

$$CV_P^2 = \frac{1}{2\left(1 + \frac{n_p^\star}{n_s^\star}\right)} \left[\frac{1 + 2\langle B_s \rangle}{n_s^\star} + \frac{1 + 2\langle B_e \rangle}{n_e^\star} \cdot \frac{k_5 k_6}{\left(k_5 + k_6 - \langle B_e \rangle f_2'(n_e^\star)\right)\left(k_5 + k_6 \frac{n_p^\star}{n_s^\star} - \langle B_e \rangle f_2'(n_e^\star)\right)} \right]. \tag{27}$$

Also for scheme 2 it is evident that $CV_P^2(\text{scheme } 2) < CV_P^2(\text{scheme } 0)$ for any choice of the model parameters. Indeed, $CV_P^2(\text{scheme } 0)$ and $CV_P^2(\text{scheme } 2)$ only differ in the denominator of the second addend in the square brackets (27), always larger than the corresponding contribute in (16) because, according to (9):

$$\begin{aligned} -\langle B_e \rangle f_2'(n_e^\star) &= \langle B_e \rangle \beta_2 h_2 \theta_2^{h_2} \frac{(n_e^\star)^{h_2 - 1}}{(\theta_2^{h_2} + (n_e^\star)^{h_2})^2} = h_2 \langle B_e \rangle \beta_2 \frac{\theta_2^{h_2}}{\theta_2^{h_2} + (n_e^\star)^{h_2}} \cdot \frac{(n_e^\star)^{h_2 - 1}}{\theta_2^{h_2} + (n_e^\star)^{h_2}} \\ &= h_2 \langle B_e \rangle f_2(n_e^\star) \cdot \frac{(n_e^\star)^{h_2 - 1}}{\theta_2^{h_2} + (n_e^\star)^{h_2}} = h_2 k_5 \frac{(n_e^\star)^{h_2}}{\theta_2^{h_2} + (n_e^\star)^{h_2}} > 0. \end{aligned} \tag{28}$$

Thus, similarly to scheme 1, also for scheme 2 the feedback on the enzyme production reduces the noise in the product fluctuations, and these results are qualitatively and quantitatively in agreement with those provided by the SHS without QSSA.

Getting in the details of (27), it comes that:

– by increasing θ_2 with respect to $n_e^\star$ ($\theta_2 \gg n_e^\star$), the effect of the feedback on the noise reduction is attenuated since, according to (28), $\langle B_e \rangle f_2'(n_e^\star) \mapsto 0$ and, straightforwardly, $CV_P^2(\text{scheme } 2) \mapsto CV_P^2(\text{scheme } 0)$; instead, by decreasing θ_2 with respect to $n_e^\star$ ($\theta_2 \ll n_e^\star$), the effect of the feedback on the noise reduction is enhanced, with $-\langle B_e \rangle f_2'(n_e^\star)$ approaching the value of $h_2 k_5$. Such a qualitative behavior for varying values of θ_2 is coherent with data shown in Fig.4, right panel, according to the ss-SSA and SHS without QSSA;

– the substrate average burst size $\langle B_s \rangle$ does not influence $\langle B_e \rangle f_2'(n_e^\star)$, which is, instead, influenced by the enzyme average burst size: high values of $\langle B_e \rangle$ proportionally provide high values of $n_e^\star$ making it so that $-\langle B_e \rangle f_2'(n_e^\star) \mapsto h_2 k_5$; on the other hand, low values of $\langle B_e \rangle$ may vanish the feedback effect in terms of noise reduction, since $-\langle B_e \rangle f_2'(n_e^\star) \mapsto 0$;

– the promoter sensitivity h_2 enhances the effect of the feedback, especially for low values of the repression threshold θ_2.

4.5. Comparison between the two feedback schemes

According to (9), the approximation in (20), provided that $k_3/k_2 \ll 1$, simplifies the equation for CV_P^2 into:

$$CV_P^2 \simeq \frac{1+2\langle B_e\rangle}{2n_e^\star}\cdot\frac{k_6}{k_5\big(1+h_2\alpha_{h_2}(n_e^\star/\theta_2)\big)+k_6}\cdot\frac{1}{1+h_2\alpha_{h_2}(n_e^\star/\theta_2)},\quad \alpha_h(x)=\frac{x^h}{1+x^h} \tag{29}$$

so that, by exploiting (22), the CV_P^2 for the two feedback schemes can be related as follows:

$$CV_P^2(\text{scheme 2}) = CV_P^2(\text{scheme 1})\cdot\frac{k_5+k_6}{k_5\big(1+h_2\alpha_{h_2}(n_e^\star/\theta_2)\big)+k_6}\cdot\frac{1+h_1\alpha_{h_1}(n_p^\star/\theta_1)}{1+h_2\alpha_{h_2}(n_e^\star/\theta_2)}. \tag{30}$$

This equation helps us to understand which of the two feedback schemes works better in view of the metabolic noise reduction. For instance, if we assume to set the feedback parameters in order to have the same ratios $n_p^\star/\theta_1 = n_e^\star/\theta_2$ and the same promoter sensitivities $h = h_1 = h_2$, then it straightforwardly comes that scheme 2 becomes always preferable to scheme 1, since:

$$CV_P^2(\text{scheme 2}) = CV_P^2(\text{scheme 1})\cdot\frac{k_5+k_6}{k_5\big(1+h\alpha_h(n_e^\star/\theta_2)\big)+k_6} \leq CV_P^2(\text{scheme 1}). \tag{31}$$

According to such a behavior, the improvements in the metabolic noise reduction coming from scheme 2 become more and more evident with respect to those coming from scheme 1 by increasing the promoter sensitivity h: Fig. 5 shows how the metabolic noise varies as a function of h, according to the setting $\theta_1 = n_p^\star$, $\theta_2 = n_e^\star$.

On the other hand, if one keeps the general setting of eq.(30), the following condition must be fulfilled in order to have $CV_P^2(\text{scheme 2}) < CV_P^2(\text{scheme 1})$:

$$(k_5+k_6)\left(1+h_1\alpha_{h_1}(n_p^\star/\theta_1)\right) < \left(k_5\big(1+h_2\alpha_{h_2}(n_e^\star/\theta_2)\big)+k_6\right)\left(1+h_2\alpha_{h_2}(n_e^\star/\theta_2)\right). \tag{32}$$

Under the hypothesis of a common promoter sensitivity $h_1 = h_2 = h$, we can easily find the domain on the parameter space $(n_p^\star/\theta_1, n_e^\star/\theta_2)$ where feedback scheme 1 is to be preferred to feedback scheme 2. In Fig. 6 such a domain for $h = 1$ is given by the purple region (and outside the opposite). By increasing the value of h, such a domain enlarges: for instance, when $h = 8$, the region where feedback scheme 1 is to be preferred to feedback scheme 2 includes both the purple and the pink regions. For a further increment of the parameter h, the enlargement progressively reduces, with the domain boundary eventually approaching the black line for $h \mapsto +\infty$. In summary, an increase in the promoter sensitivity provides more benefits to the feedback from the product with respect to the feedback from the enzyme, in terms of enlarging the parameter design space.

5. Conclusions

In this work, we presented a comparison between two feedback schemes applied to a basic enzymatic reaction network. Performances have been evaluated in terms of metabolic noise reduction,

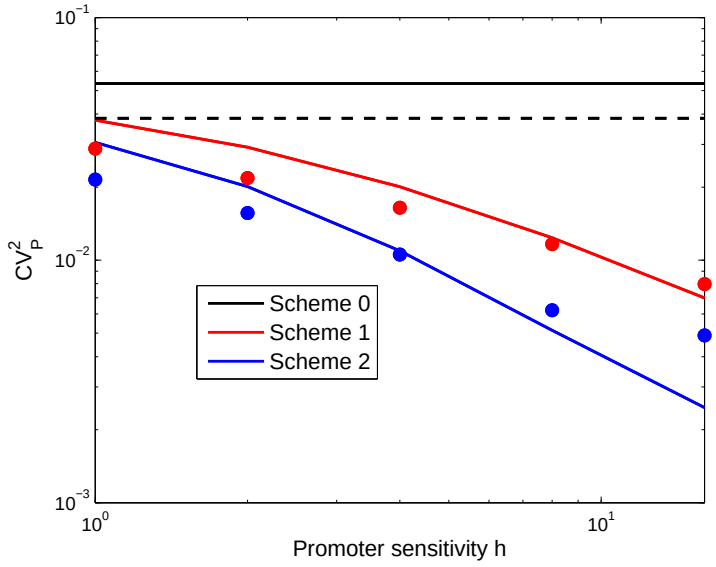

Fig. 5. *Metabolic noise for different values of the promoter sensitivity, according to constraints $\theta_1 = n_p^\star$, $\theta_2 = n_e^\star$ and $h_1 = h_2 = h$. The solid lines are referred to the SHS formulation. The dotted line (scheme 0) and the circles (feedback schemes 1 and 2) are obtained by means of the slow-scale Stochastic Simulation Algorithm.*

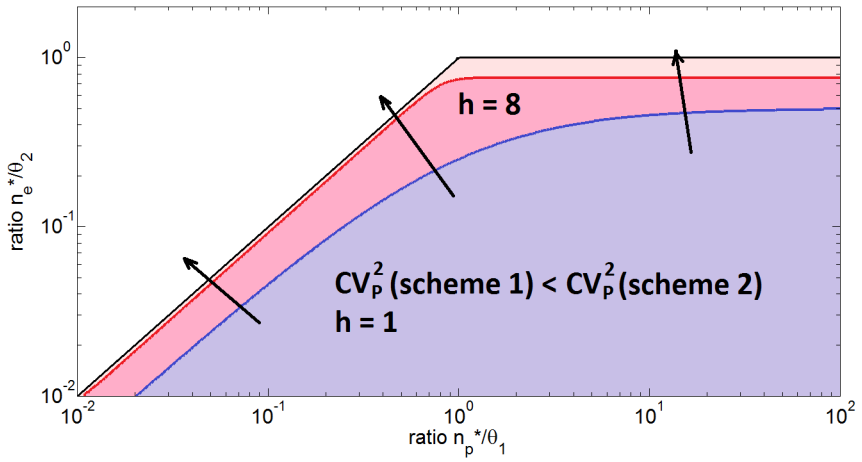

Fig. 6. *Domain of $(n_p^\star/\theta_1, n_e^\star/\theta_2)$ where feedback scheme 1 provides a CV_P^2 smaller than scheme 2. The purple region refers to the case $h = 1$. By increasing h, the boundary of such a region moves according to the arrows, eventually approaching the black line. The red line refers to such a boundary for the case $h = 8$.*

where the noise is measured in terms of coefficient of variation of the reaction product around its steady-state average value. The obtained simulations confirm general experimental results, including an overall noise reduction effect for both feedback schemes [16, 17], with a pivotal role played by the promoter sensitivity, which enhances the noise reduction. The latter effect (known also as

ultrasensitive regulation) has been experimentally shown to hold also in different systems biology frameworks, e.g. improving flux adaptation in unbranched metabolic pathways [31] and noise rejection in signaling cascades [32]. The case where the enzyme production is not regulated is outperformed by the two regulation schemes (product-feedback and enzyme-feedback), as shown by evaluating the noise by means of numerical simulation (ss-SSA) and by analytical computations exploiting the Stochastic Hybrid Systems (SHS) framework combined with the Quasi Steady-State Approximation (QSSA). Analytical results suggest the parameter settings according to which one of the two feedback schemes provides the best results with respect to metabolic noise reduction.

Acknowledgements

Pasquale Palumbo is supported by the MIUR grant SysBioNet - Italian Roadmap for ESFRI Research Infrastructures, SYSBIO Centre of Systems Biology, Milan and Rome, Italy. Abhyudai Singh is supported by the National Science Foundation Grant DMS-1312926, University of Delaware Research Foundation (UDRF) and Oak Ridge Associated Universities (ORAU).

6. References

[1] D.E. Cameron et al, A brief history of synthetic biology, *Nat. Rev. Microbiol.*, 12, 381–390, 2014.

[2] D. Del Vecchio, and E. D. Sontag, Synthetic biology: A systems engineering perspective, *Control Theory and Systems Biology*, 101–124, 2009.

[3] D. Del Vecchio, A. J. Ninfa, and E. D. Sontag, Modular cell biology: retroactivity and insulation, *Molecular systems biology, 4.1, 161, 2008.*

[4] D. Del Vecchio, Modularity, context-dependence, and insulation in engineering biological circuits, *Trends in Biotechnology*, 33(2), 111–119, 2015.

[5] G. Stephanopoulos, A. Aristidou, J. Nielsen, *Metabolic Engineering: Principles and Methodologies*, Academic Press, San Diego, CA, 1998.

[6] W.J. Holtz, J.D. Keasling, Engineering static and dynamic control of synthetic pathways, *Cell*, 140, 19–23, 2010.

[7] A. Zaslaver, A. Mayo, R. Rosenberg, P. Bashkin, H. Sberro, M. Tsalyuk, M. Surette, U. Alon, Just-in-time transcription program in metabolic pathways, *Nat. Genet.* 36, 486–491, 2004.

[8] U. Alon, *An Introduction to Systems Biology: Design Principles of Biological Circuits*, Chapman and Hall/CRC, 2006.

[9] D.H. Calhoun, G.W. Hatfield, Autoregulation: a role for a biosynthetic enzyme in the control of gene expression, *Proceedings of the National Academy of Sciences* 70.10 (1973): 2757-2761.

[10] D.A. Oyarzun, J.-B. Lugagne, G.-B. Stan, Noise propagation in synthetic gene circuits for metabolic control, *ACS Synthetic Biology*, 2014.

[11] A. Borri, P. Palumbo, A. Singh, Metabolic noise reduction for enzymatic reactions: the role of a negative feedback, *Proceedings of the 54th IEEE Conference on Decision and Control (CDC 2015)*, Osaka, Japan, pp. 2537–2542, 2015.

[12] T. Tianhai, K. Burrage, Stochastic models for regulatory networks of the genetic toggle switch, *Proceedings of the National Academy of Sciences* 103.22, 8372-8377, 2006.

[13] Y. Dublanche, K. Michalodimitrakis, N. Kmmerer, M. Foglierini, L. Serrano, Noise in transcription negative feedback loops: simulation and experimental analysis, *Molecular systems biology* 2(1), 41, 2006.

[14] S. Hooshangi, R. Weiss, The effect of negative feedback on noise propagation in transcriptional gene networks, *Chaos: An Interdisciplinary Journal of Nonlinear Science* 16.2, 2006.

[15] H. Zhang, Y. Chen, Y. Chen, Noise propagation in gene regulation networks involving interlinked positive and negative feedback loops, *PloS one* 7.12, 2012.

[16] A. Becskei, L. Serrano, Engineering stability in gene networks by autoregulation, *Nature*, 405, 590–593, 2000.

[17] V. Shahrezaei, J.F. Ollivier, P.S. Swain, Colored extrinsic fluctuations and stochastic gene expression, *Mol. Syst. Biol.*, 4, 196-1–196-9, 2008.

[18] N.G. van Kampen, *Stochastic Processes in Physics and Chemistry*, North Holland, third edition, 2007.

[19] A. Borri, F. Carravetta, G. Mavelli, P. Palumbo, Block-tridiagonal state-space realization of Chemical Master Equations: A tool to compute explicit solutions, *Journal of Computational and Applied Mathematics*, Vol. 296, 410–426, 2016.

[20] D. T. Gillespie, Exact Stochastic Simulation of Coupled Chemical Reactions, *The Journal of Physical Chemistry* 81(25), 2340–2361, 1977.

[21] Y. Cao, D. Gillespie, L. Petzold, The slow-scale stochastic simulation algorithm, *J. Chem. Phys.* 122, 014116, 2005.

[22] Y. Cao, D. Gillespie, L. Petzold, Accelerated stochastic simulation of the stiff enzyme-substrate reaction, *J. Chem. Phys.* 123, 144917, 2005.

[23] J.P. Hespanha, A. Singh, Stochastic models for chemically reacting systems using polynomial stochastic hybrid systems, *Int. J. of Robust and Nonlinear Control* 15, 669-689, 2005.

[24] M. Soltani, P. Bokes, Z. Fox, A. Singh, Nonspecific transcription factor binding can reduce noise in the expression of downstream proteins, *Phys. Biol.*, **12** (2015) 055002.

[25] A. Singh, J.P. Hespanha, Approximate moment dynamics for chemically reacting systems, *IEEE Transactions on Automatic Control* 56, 414-418, 2011.

[26] M. Soltani, C. Vargas, A. Singh, Conditional moment closure schemes for studying stochastic dynamics of genetic circuits. *IEEE Transactions on Biomedical Circuits and Systems*, 9(4), 518–526, 2015.

[27] I. Golding, J. Paulsson, S. Zawilski, E. Cox, Real-time kinetics of gene activity in individual bacteria, *Cell* 123, 1025-1036, 2005.

[28] N.E. Buchler, F.R. Cross, Protein sequestration generates a flexible ultrasensitive response in a genetic network. *Molecular systems biology* 5(1), 272, 2009.

[29] L. Segel, On the validity of the steady state assumption of enzyme kinetics, *Bull. Math. Biol.* 50, 579–593, 1988.

[30] A.M. Bersani, E. Bersani, L. Mastroeni, Deterministic and stochastic models of enzymatic networks - applications to pharmaceutical research, *Computers and Mathematics with Applications* 55, 879-888, 2008.

[31] D.A. Oyarzun, G.-B. Stan, Design tradeoffs in a synthetic gene control circuit for metabolic networks, *Proc. 31st Am. Control Conf.*, 2743–2748, 2012.

[32] M. Thattai, A. van Oudenaarden, Attenuation of noise in ultrasensitive signaling cascades, *Biophys. J.*, 82, 2943–2950, 2002.